Design and Analysis of Submarine Radome

N. V. Srinivasulu, Safeeruddin Khan and S. Jaikrishna

Abstract Submarine antenna is used for communication by RF system. It is protected by radomes. Radomes are the electromagnetic (EM) windows that protect microwave subsystems from the environmental effects. Low-observable radomes are usually made of E-glass/epoxy composite due to its low dielectric constant which is necessary not to interfere EM wave transmission characteristics. Aramid fibers have lower dielectric constant and higher strength than those of E-glass fiber. The dielectric strength constant and loss tangent were measured of the E-glass epoxy and aramid epoxy materials. Increasing the performance of antenna depends upon the proper selection of material to withstand under the water applications, composite materials owing to their high strength to weight ratio, high stiffness and better corrosion resistance are potential source for under water applications. ANSYS, a Finite Element software package was used to analyze the problem. The radome design and finite element analysis validation concluded by conducting the pressure test on radome. The modal analysis is also carried out on radome to check for the natural frequency of the radome. So that resonance does not occur if the natural frequency of the radome coincides with the excitation frequency of the submarine.

Keywords Submarine radome · Finite element analysis · Composites

N. V. Srinivasulu (✉) · S. Khan
Department of Mechanical Engineering, Chaitanya Bharathi Institute of Technology, Hyderabad 500075, Andhra Pradesh, India
e-mail: vaastusrinivas@gmail.com

S. Jaikrishna
Narasimhareddy Engineering College, Hyderabad, Andhra Pradesh, India

S. S. Khangura et al. (eds.), *Proceedings of the International Conference on Research and Innovations in Mechanical Engineering*, Lecture Notes in Mechanical Engineering, DOI: 10.1007/978-81-322-1859-3_2, © Springer India 2014

1 Introduction

Radar dome, or usually called radome, is usually placed over the antenna as an antenna protector. The basic function of a radome is to form a protective cover between an antenna and the environment with minimal impact on the electrical performance of the antenna. Under ideal conditions, a radome is electrically invisible. How well a radome accomplishes this depends on matching its configuration and materials composition to a particular application and radio frequency range.

Radomes can be found protecting a wide range of outdoor terrestrial and shipboard communications systems and radar installations as well as airborne avionics system antennas. The proper selection of a radome for a given antenna can actually help to improve overall system performance by doing the following:

1. Maintaining alignment by eliminating wind loading and allowing for all-weather operations by protecting the system from rain, snow, hail, sand, salt spray, insects, animals, UV damage, and wide temperature fluctuations.
2. Providing shelter for installation and maintenance personnel.
3. Preventing visual observation of system (security).
4. Minimizing downtime and extending component and system operating life.

Radomes can be classified into ground-based, naval, and airborne radomes.

Historically, a variety of materials have been used for constructing radomes, including balsa and plywood in early structures. Modern ground-based and ship-based radomes are manufactured using composite materials such as fiberglass, quartz, and aramid fibers held together with polyester, epoxy, and other resins, such as the one shown. Foam and honeycomb cores are often added between inner and outer “skins” of the radome to function as a low-dielectric-constant spacer material providing structural strength and rigidity.

2 Radome

2.1 Radome Configuration

Several radome configurations are used to minimize RF reflections, including electrically thin, half-wave, A-sandwich, C-sandwich, and others. The best configuration for a particular application depends on the mechanical requirements and operating frequency.

A radome that is electrically thin (less than 0.1 wavelengths) as shown will generally deliver good RF performance. This is because signal reflections at the free-space/dielectric boundary are canceled out by out-of-phase reflections from the dielectric/free-space boundary on the other side of the dielectric material.

Signal losses are low, and the net transmission from an electrically thin dielectric laminate is very high. Unfortunately, electrically thin radomes provide very little thermal insulation and are not suitable for locations with wide temperature extremes and a requirement for controlled temperatures.

Another radome approach that works well is a configuration based on the half-wavelength-thick solid laminate shown in Fig. 5. It is similar to the electrically thin configuration because the reflections cancel out. The wave travels 180° through the laminate, is reflected with a phase shift of −180°, and travels another 180° on the return trip to achieve the net 180° phase shift required for cancelation. Performance of the same laminate is described in Fig. 4 at higher frequencies (through 35 GHz) where it is 0.5 wavelengths thick.

A-sandwich radome configuration consists of low dielectric foam or honeycomb core sandwiched between two thin laminates. Its operation is similar to the half-wavelength-thick solid laminate. However, it is 0.25 wavelengths thick because the reflection coefficients from the skins have the same amplitude and phase. The round trip for the reflection from the second skin is 0.5 wavelengths. The reflections, which are 180°, are out of phase.

A C-sandwich radome consists of three skin layers and two foam layers. The thickness of each foam layer, and possibly the skins, can be tuned for optimal RF performance in the bands of interest. This can lead to many potential construction combinations that can provide good RF performance and high mechanical strength. C-sandwich constructions provide better performance than A-sandwich radomes; however, the added complexity increases material and labor costs.

2.2 *Radome Wall Diffraction*

The uniform radome wall represents 90–96 % of a radome surface. Therefore, it has to be designed carefully. Any A-sandwich consists typically of three layers as demonstrated in Fig. 1:

(a) inside skin
(b) foam core
(c) outside skin (with hydrophobic coating)

Figure 1 shows that the electromagnetic (EM) wave can easily transmit throughout the material layers of foam core in sandwich construction. The transmission of EM waves through any sandwich can be calculated as the diffraction of EM energy at boundaries between areas of different dielectric properties. Based on the knowledge of the EM properties of the materials like dielectric constant and loss factor, it is possible to develop a transmission matrix T for every single boundary depending on the incidence angle, frequency, and polarization of the EM wave and to calculate the transmission loss. Figure 1 shows the one-way transmission loss for an EM wave. Over frequency at 0°, 20°, and 40° incidence angle and linear TE polarization for a typical A-sandwich designed for C-band weather

Fig. 1 Installation of radome over the antenna

radar applications. In Fig. 1, the parabolic antenna is protected by the radome. These radome only can help to improve the performance of radome underwater-depth applications and protects from the environment.

2.3 Structural Support

Although radomes are used extensively on airframes and missiles, this section focuses specifically on support structures for terrestrial and shipboard systems. Ground and shipboard radomes can range in size from very small antenna covers to massive structures.

Self-supporting radomes are usually based on an A-sandwich configuration. They are made of rigid sections that are bolted or latched together. If phase delay and insertion loss through the seam is matched to the rest of the radome, the seam becomes largely invisible to the EM wave front. Unlike other radome types mentioned in this article, A-sandwich radomes require no air blowers to maintain pressure and are not dependant on electrical power to maintain their electromagnetic or structural performance. A-sandwich radomes generally have lower overall operation and maintenance costs.

Inflatable radomes are made of electrically thin dielectric cloth. By being electrically thin, they are capable of achieving very low loss over wide bandwidths. The trade-off for high performance, however, is that they require a constant supply of air. Inflatable radomes must be supported by internally generated air pressure, which is supplied by air blowers or air compressors. In order to maintain adequate air pressure, inflatable radomes must be equipped with airlocks at all doors and a standby power supply to operate the blowers at all times and under all environmental conditions. Should the membrane suffer damage or whether power is interrupted, it is possible for the radome to deflate and collapse. Operating and maintenance costs for this type of radome usually exceed those all other radome types. Metal space frame radomes support the window portion of the radome consisting of the electrically thin, half-wave, or A-sandwich configuration, often in the shape of a geodesic dome. The window portion typically has very low loss. However, 10 signal blockages from the frame reduce system gain and reflect noise back into the system. Because the frame reflects and refracts the RF wave front, it increases side lobe levels. A method used to prevent large side lobes is the use of a quasi-random frame pattern. The quasi-random pattern is also used to minimize side lobes for the other support structure types. In contrast to metal space frame radomes, dielectric space frame radomes are supported by dielectric members who are somewhat electrically transparent. However, the wave front is phase delayed as it passes through the dielectric support, alternating between in and out of phase, depending on frequency. If the delay is 180° out of phase, with the phase of the incident signal, the energy that passes through the frame subtracts from the gain. This leads to a frequency-dependant sinusoidal ripple in the insertion loss, and the lost energy goes into the side lobes. This makes dielectric space frame radomes best suited to systems that operate at less than 1 GHz. Both types of space frame radomes usually require the use of air blowers or compressors in order to maintain and enhance the structural integrity of their thin membrane coverings during windy conditions. Failure to maintain positive pressure can result in membrane damage and failure.

2.4 Impact of Incident Angle

All of the plots and explanations thus far show reflections at normal incidence. Typically, an EM wave hits the radome surface at an oblique angle, or in the case of a spherical radome a continuous range of oblique angles. The transmission characteristics of the radome change with the wave incidence angle and polarization. Electric fields that are parallel to the plane of incidence have much higher transmission than fields that are perpendicular to the plane of incidence. Aerodynamic radomes used on aircraft and missiles often see high incidence angles. This can result in large amounts of axial ratio degradation for circularly polarized antennas and higher insertion loss. EM wave fronts from parabolic antennas located inside spherically shaped radomes see low incident angles at the center of the wave front. Out on the edges, however, the incident angle becomes higher. If the antenna illumination pattern is symmetric and the antenna is placed at the center of the spherical radome, the symmetric shape of the radome cancels out axial ratio degradation from the oblique incidence angles seen by the antenna. Composites are gaining wider acceptance for use on onboard warships and submarines due to number of advantages, viz., high strength-to-weight ratio, ability to be molded into complex shapes, better EMI performance, and absence of corrosion palliatives that otherwise are source for electronic and magnetic signature. Composite materials made from E-glass fibers and epoxy resins have become very popular as a radome material due to its outstanding transparency to microwaves and having good mechanical properties. The increasing popularity of the material for underwater application are posing great difficulties to the designer to select right combination of composition and shape of radome due to the complex nature of the structure and the loading conditions for the useful operation life.

Mechanical properties of composite materials are influenced by several factors like reinforcement, fiber orientation, adhesion, composition, manufacturing process, etc. Conducting the tests on standard specimens and evaluating mechanical properties is the most important aspect in the design of composite material applications. The ASTM guidelines were followed in testing and preparation of standard test specimens. The micromechanics and failure mechanism of composite material is very complex compared to the conventional isotropic materials. Depending on the reinforcement, composition content, and its percentage, appropriate theory and failure mechanism can be considered for designing the radome.

Finite element analysis of radome design is carried out using (Analysis System) ANSYS, a FEA software package. Geometrical model of radome is generated as per radome sketch. Suitable elements are selected, and optimum size of mesh is generated. Material properties, evaluated from tests, are assigned. Boundary conditions and load cases are applied to complete the preprocessing stage. The post-results obtained after FE analysis are compared with design requirements. The main objective of this project is to develop composite radome that protects the electronic equipment from high water pressure and transparent to EM waves.

In Fig. 2, we can see the shape of radome assembled with the bolts and nuts by holes.

The geometric shape of the radome is a cylindrical barrel covered with a hemispherical dome at the top. It has a circular plate at the bottom end of the cylinder having M6-size holes which acts as a flange. The radome is secured to the submarine structure with M6 bolts on its flange. Radome is made of sandwiched construction with glass-reinforced plastic (GRP) as sheet material and syntactic foam as core. E-glass woven fabric and epoxy resin are used after FE analysis compared with design requirements.

2.5 Functions of the Radome

The functions of the radome are as follows:

1. The radome protects the installation from the deteriorating effects of environment and extends the durability of antenna and other equipment.
2. The overall performance of the antenna will be increased with the use of radome.
3. FRP radome helps to have overall economy and weight reduction.
4. A radome permits the airborne antenna to function with good efficiency under high head of the water over the submarine.

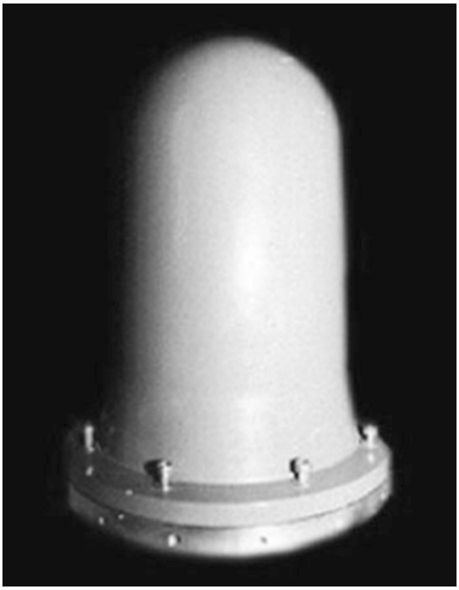

Fig. 2 Submarine radome

3 Construction and Materials

Advanced composites and special products are made from reinforcements such as fiberglass, quartz, graphite, and Kevlar® along with matrices such as polyester, epoxies, and cyanate ester. We also use core materials such as honeycomb (e.g., fiberglass, aluminum, and graphite) and foams (e.g., polyisocyanate and thermoformable cores). Depending on the application, these parts are oven-cured at temperatures up to 400 °F or in autoclaves, which require high-pressure cures at high temperatures. Other materials are also available for special applications. Regardless of the application(s), we can select the right combination of reinforcement and matrix to meet requirements.

All of these products include excellent EM performance for their intended applications, providing up to 98 % transmission efficiency depending on frequency. Some typical examples include the following: Naval radomes are used in shipboard radar applications, high-data-rate communications systems, gunfire control, and high-bandwidth data link terminals.

A probe by accident into the field of thermosetting polymers has brought about a quantum growth in its basic as well as technological aspects. The synthetic thermosetting polymers with the combinational properties of the existing conventional high-strength polymers and glass fibers with a variety of filler materials have altogether offered a new field of research. The review of work presented here reveals that large effort has gone into the understanding of the mechanical, thermal, and physical properties of thermosets. A thorough literature search reveals that there are no systematic studies on mechanical properties of thermosetting composites. There is ample scope for fabrication of newer composites with different weight fractions of glass fiber and PET in polymers and their characterization for physical, mechanical, and thermal properties. A variety of filler materials have altogether offered a new field of research.

4 Hybrid Composites

A thorough literature search reveals that there are no systematic studies on mechanical properties of thermosetting composites. There is ample scope for fabrication of newer composites with different weight fractions of glass fiber and fillers in polymers and their characterization for physical, mechanical, and thermal properties.

In this thesis, a wealth of data on mechanical properties of polymer glass filler composites has been generated. These data are useful for material technologists, mechanical engineers, and defense engineers, who can make use of this database for the generation of new materials for specific application. In that respect, it has been used in GF and virgin PET fibers in the form of woven mat and epoxy as matrix. Laminates are obtained from vacuum bag molding technique. Tests were carried out to evaluate physic-mechanical and thermal properties according to ASTM standards Table 1.

5 Analysis of Submarine Radome

The following different load cases are considered for designing radome:

Case (i) Water head pressure acting on radome (due to under water)

Water head pressure acting on radome $(p) = \rho gh$.

Density of seawater at average temperature of 25 °C $(\rho) = 997.0479\ \text{kg/m}^3$

Radome depth in water $(h) = 490$ m, $P = 997.0479*9.91*490 = 4.7920*10E6/\text{Nm}^2 = \text{P} = 48$ bar

The maximum operating depth (popularly called the never-exceed depth) is the maximum depth at which a submarine is allowed to operate under any conditions. World War II German U-boats generally had collapse depths in the range of 200–280 m (660–920 ft). Modern nuclear attack submarines like the American Seawolf class are estimated to have a test depth of 490 m which would imply (see above) a collapse depth of 730 m (2,400 ft)

Following assumptions are made to analyze the model.

1. Water pressure acting on the periphery of the radome.

Table 1 Physical dimensions of radome

Physical dimensions	Values in mm
Diameter	1,651
Height	1,384.3
Hole diameter	50
Thickness	275

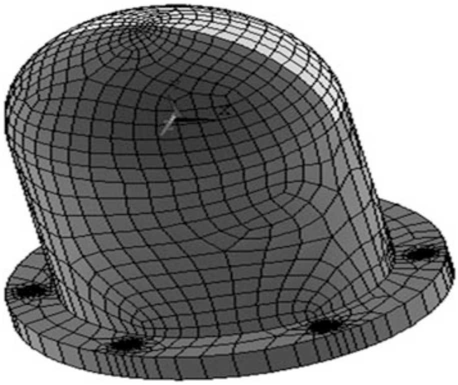

Fig. 3 Meshing of radome

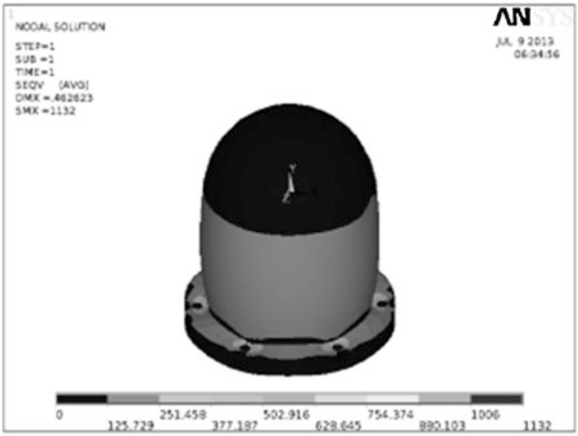

Fig. 4 Displacement vector sum

2. Material properties taken for E-glass/epoxy fiber reinforced plastic with fiber orientation of 0 and 90°.
3. Mounting flange of radome of assumed rigid body.

Static analysis:
ANSYS has been used for the finite element analysis of the radome. Linear static analysis is carried out to find out the structural response of the model. The area of radome is meshed with shape tetra and free meshed and is shown in Fig. 3.

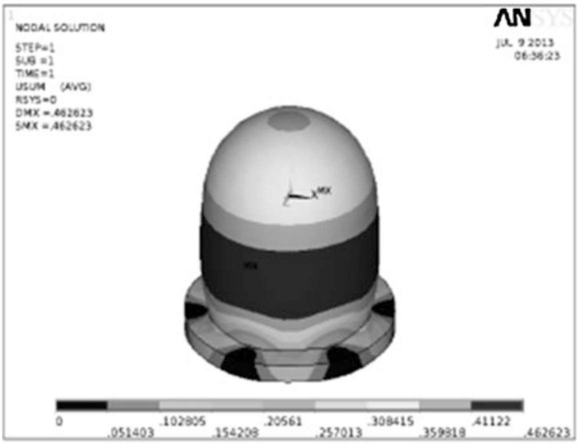

Fig. 5 Von Mises stress of aramid epoxy

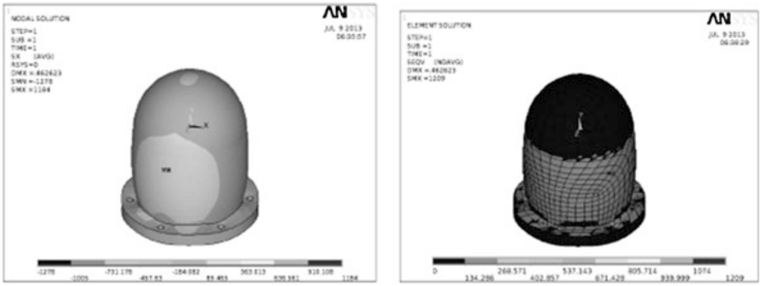

Fig. 6 *X*-component and von Mises stress of aramid epoxy

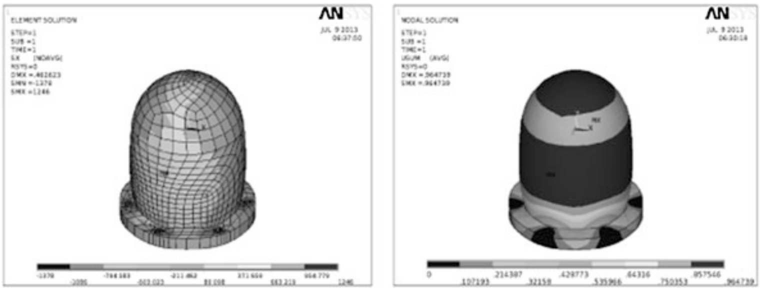

Fig. 7 Element stress in *x*-direction and displacement vector sum of E-glass epoxy

Figure 4 shows the maximum displacement vector sum is 0.462623 mm of aramid epoxy material. Maximum displacement occurs at the center of the dome

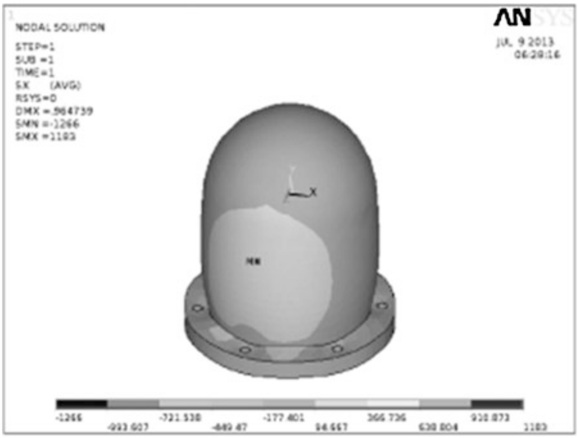

Fig. 8 Stress component in *x*-direction

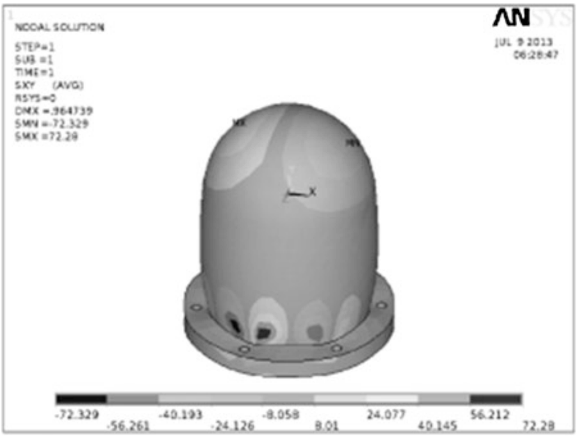

Fig. 9 Shear stress in *x*-direction

which is shown in figure with the indication of MX. This deflection does not have much effect on the radome.

Figure 5 shows the maximum stress occurs at the corners of the hole which is 1,132 MPa. The ultimate tensile strength of material is 1,377 MPa which is less than resulted stress. So this design is in safe limit in static mode. The high stresses are occurring only at the corner of hole. The corner hole stress can be reduced by stress concentration factor. The thickness of the material decreases which also reduces the weight.

Figure 6 shows the tensile stress in *x*-direction of the aramid epoxy is 1,184 MPa, but the actual strength of tensile stress in *x*-direction is 1,377 MPa. In case of comparing tensile stress in *x*-direction, also the design is in safe limit. Figure 7 shows the element stress in *x*-direction of aramid epoxy is 1,246 MPa. It is lower compared to ultimate tensile strength of aramid epoxy resin (Fig. 7). The elemental von Mises stress is 1,209 MPa which is below than ultimate tensile

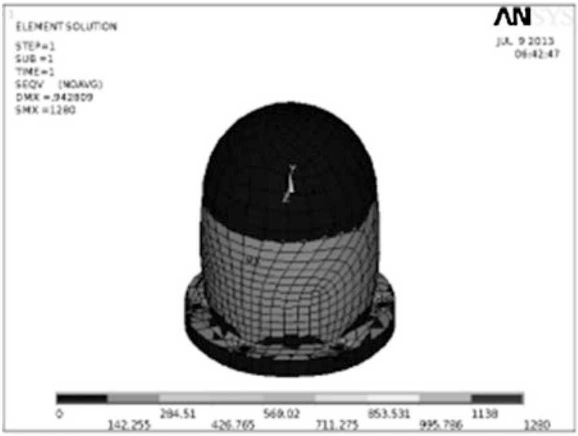

Fig. 10 Von Mises stress of E-glass epoxy

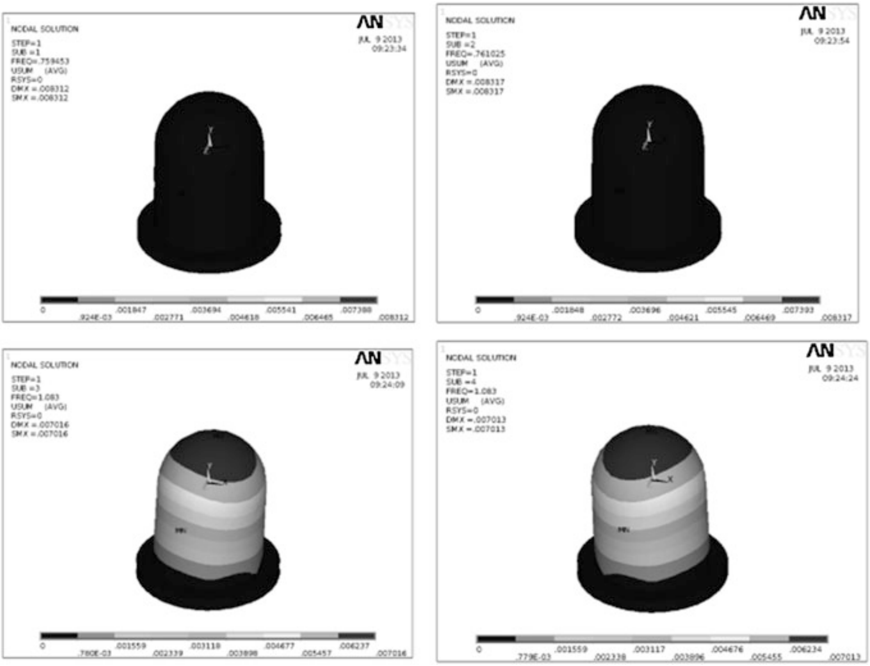

Fig. 11 Frequency and mode shape of substeps 1, 2, 3, and 4

strength of aramid epoxy. So this design is safe. The displacement vector sum of E-glass epoxy is 0.964739 mm, which is under the pressure of 48 bar. The maximum deformation occurs at the top and center of the radome. The constrained portion of hole has minimum deflection.

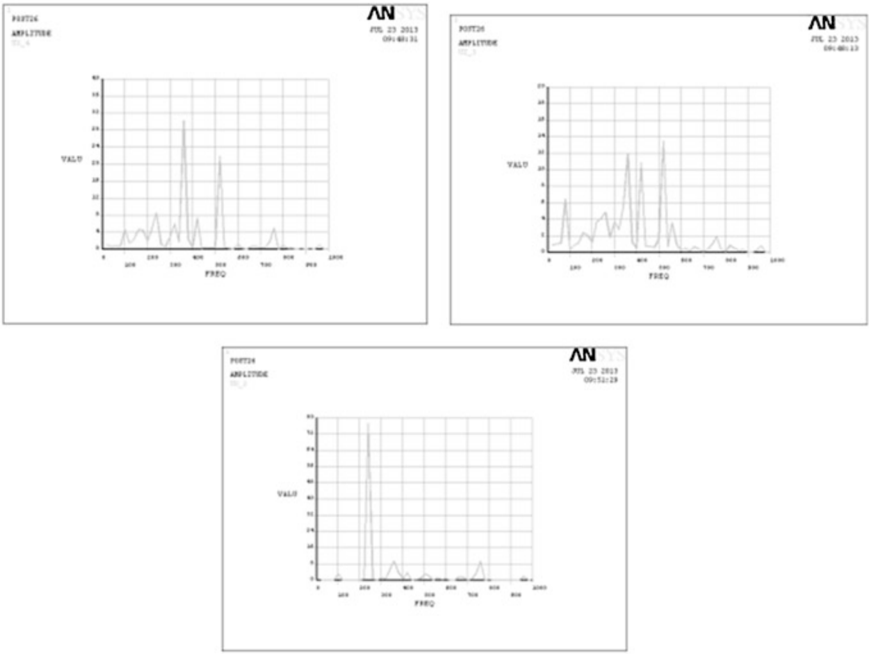

Fig. 12 Displacement (UX) graph between amplitude versus frequency for first step at node 665 for frequency 360 Hz

Figure 8 shows the resulted stress in x-direction is 1,183 MPa which lower than the ultimate tensile strength of E-glass epoxy (1,243 MPa). The maximum stress occurs at the edges of the hole.

The result of shear stress in x-direction is 72.28 MPa, but the actual shear strength capability of E-glass epoxy is 73 MPa. By comparing the shear stresses, both are closest with each other. It cannot be say as a safe limit. It may have chance to failure (refer Fig. 9). Figure 10 shows the von Mises stress of E-glass epoxy is 1,280, but the ultimate tensile strength of E-glass epoxy is 1,243. It cannot be safe design because the resulted stress reaches the ultimate tensile strength.

Modal analysis was used to determine the vibration characteristics (natural frequencies and mode shapes) of a structure or a machine component while it is being designed. It also can be a starting point for dynamic analysis, such as a transient dynamic analysis, a harmonic response analysis, or a spectrum analysis.

Figure 11 shows the frequency of aramid epoxy is 0.759453 Hz and deflection is 0.008312 for step 1; frequencies and modes of shape for aramid epoxy are 0.751025 and 0.008317 for step 2; frequency and modes of shape for aramid epoxy are 1.083 and 0.007016 for step 3; and frequency and modes of shape for aramid epoxy are 1.083 and 0.007013 for step 4. Maximum deflections occur at the top of the dome. The frequencies of each substep increase slightly. The frequencies of

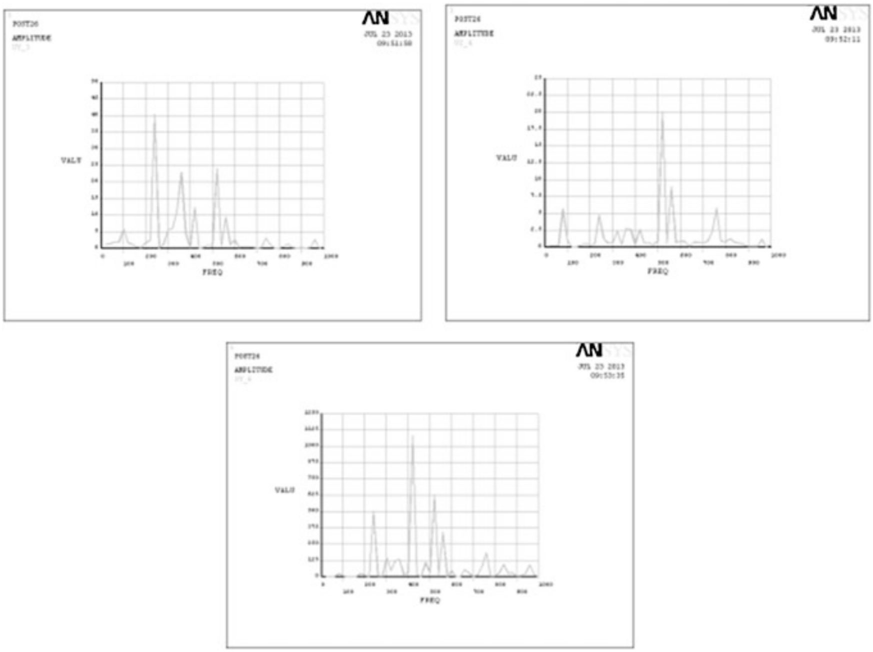

Fig. 13 Displacement in *y*-direction is for last substep at node 1,269

aramid epoxy are low and mode shapes deflections. The maximum frequency in all substep is 2.3489 which less than four times of natural frequencies.

Harmonic analysis is a branch of mathematics concerned with the representation of functions or signals as the superposition of basic waves, and the study of and generalization of the notions of Fourier series and Fourier transforms. In the past two centuries, it has become a vast subject with applications in areas as diverse as signal processing, quantum mechanics, and neuroscience. The term "harmonics" originated in physical eigenvalue problems, to mean waves whose frequencies are integer multiples of one another, as are the frequencies of the harmonics on stringed musical instruments, but the term has been generalized beyond its original meaning.

6 Results and Discussions

The von Mises stress of element is 1,280 which reaches the ultimate tensile strength of E-glass epoxy which may fail. So aramid epoxy material is under the hydrostatic pressure of 48 bar. The dielectric constant and loss tangent of the aramid/epoxy composite measured by the free-space measurement method were 3.742 and 0.018 E-glass/epoxy composite (4.686 and 0.015) aramid preferable because it has low dielectric constant and loss tangent. Maximum displacement

Table 2 Summary of results for epoxy material

Components	E-glass epoxy		Aramid epoxy	
	Ultimate tensile strength (MPa)	Resultant stress (MPa)	Ultimate tensile stress (MPa)	Resultant stress (MPa)
Stress in *x*-direction	1,243	1,183	1,377	1,184
Von Mises stress of nodal	1,260	1,173	1,392	1,132
Von Mises stress of element	1,243	1,280	1,377	1,209
Shear stress in *xy*-direction	73	72.8		

vector sum is 0.964 mm of E-glass epoxy material. Maximum displacement sum of aramid epoxy is 0.462 mm. which is less than that of E-glass epoxy material. In modal analysis, the maximum frequency value is 2.018 Hz. The natural frequency of the radome is less than four times the excitation frequency so that resonance does not occur. Displacement in *z*-direction is for substep 1 at node 1,269. Maximum amplitude is 13 mm at the frequency of 520 Hz as shown in Fig. 12. Figure 13 shows displacement in *x*-direction is for last substep. Maximum amplitude is 78 mm at the frequency of 250 Hz.

Maximum amplitude is 40 mm at the frequency of 250 Hz. Displacement in *z*-direction is for last substep at node 1,269. Maximum amplitude is 20 mm at the frequency of 520 Hz. Figure 13 shows stress in *y*-direction is for substep 1 at node 156. Maximum amplitude is 1,000 mm at the frequency of 420 Hz Table 2.

7 Conclusions

1. The high stresses are occurring only at the corner of hole. The corner hole stress can be reduced by stress concentration factor method.
2. Deformation and stress values obtained of E-glass epoxy from FE analysis are within the safe limits.
3. Conducting pressure test on radome verified the design aspects and validated the FE analysis.
4. To improve the electrical performance of the radome without compromising the mechanical properties hybrid composites to be considered in futuristic radome development.

References

Bourasseaua N, Moulina E, Delebarrea C, Bonniaub P Radome health monitoring with Lamb waves: experimental approach. aIEMN, UMR CNRS 9929, OAE Department, Universite′ de Valenciennes

Cady WM, Karelitz MB, Turner LA (1948) Radar scanners and Radomes. MIT University, New York
Choi I, Kim JG, Lee DG, Seo S (2011) Aramid/epoxy composites sandwich structures for low-observable radomes. School of Mechanical Aerospace and Systems Engineering, Korea Advanced Institute of Science and Technology
Chandrupatla TR, Belegundu AD (2011) Introduction to finite elements in engineering, 4th edn
DiCarlo A, Chung KH (2013) Radome-enclosed antenna's temperature and velocity fields. MITRE Corporation, Bedford
Gates PJ, Lynn NM (1990) Ships, submarines & the sea, vol 2. Brassey's, London
Harris B (1999) Engineering composite materials, 2nd edn
Joubert PN (2004) Some aspects of submarine design. Australian Government, Department of Defense
Kim PC, Lee DG (2009) Composite sandwich constructions for absorbing the electromagnetic waves. Department of Mechanical Engineering, Korea Advanced Institute of Science and Technology
Naito K, Kagawa Y, Kurihara K Dielectric properties and noncontact damage detection of plain-woven fabric glass fiber reinforced epoxy matrix composites using millimeter wavelength microwave. Research Center for Advanced Science and Technology, The University of Tokyo
Oh J-H, Oh K-S, Kim C-G, Hong C-S (2004) Design of radar absorbing structures using glass/epoxy composite containing carbon black in X-band frequency ranges. Division of Aerospace Engineering, Department of Mechanical Engineering, Korea Advanced Institute of Science and Technology, p 373
Satheesh Kumar Reddy P, Nagaraju C, Hari Krishna T (2012) Optimum design and analysis of filament wound composite tubes in pure and combined loading, vol 1(8). ISSN: 2278-0181
Sun CT (2000) Strength analysis of unidirectional composite laminates
Timoshenko SP, Gere JM (1963) Theory of elastic stability, 2nd edn. Mc Graw-Hill Book Company, New York

http://www.springer.com/978-81-322-1858-6

Proceedings of the International Conference on
Research and Innovations in Mechanical Engineering
ICRIME-2013
Khangura, S.S.; Singh, P.; Singh, H.; Brar, G.S. (Eds.)
2014, XV, 682 p. 358 illus., Hardcover
ISBN: 978-81-322-1858-6